RSC Advances

First Light-Emitting Electrochemical Cell with [Ag(I)(N^N)(P^P)] type Complex

Journal:	*RSC Advances*
Manuscript ID	RA-ART-07-2015-012921.R3
Article Type:	Paper
Date Submitted by the Author:	22-Oct-2015
Complete List of Authors:	Moudam, Omar; University of Bangor, School of Electronic Engineering Tsipis, Athanasios; University of Ioannina, Department of Chemistry Kommanaboyina, Srikanth; University of Bangor, Chemistry Horton, Peter; University of Southampton, School of Chemistry Coles, Simon; Southampton, Chemistry
Subject area & keyword:	Inorganic materials < Materials

First Light-Emitting Electrochemical Cell with [Ag(I)(N^N)(P^P)] type Complex**

Omar Moudam,[a] Athanassios C. Tsipis,[b]* Srikanth Kommanaboyina,[c] Peter N. Horton,[d] Simon J. Coles[d]*

[a]School of electronic engineering, University of Bangor, Dean St, LL57 1UT, Bangor, UK, E-mail: omoudam@yahoo.co.uk

[b]Laboratory of Inorganic and General Chemistry, Department of Chemistry, University of Ioannina, 451 10 Ioannina, Greece, E-mail: attsipis@uoi.gr

[c]School of Chemistry, University of Bangor, LL57 2UW, Bangor, UK

[d]EPSRC National Crystallography Service, School of Chemistry, University of Southampton, Highfield, Southampton, SO17 1BJ, UK

* Corresponding authors

ABSTRACT: A new heteroleptic complex formulated as [Ag(I)(Bipy)(POP)]BF_4 (Bipy = 2,2'-Bipyridine; POP = bis[(2-diphenylphosphino)phenyl]ether) was synthesized and characterized by NMR and X-ray crystallography. The complex adopts tetrahedral coordination geometry. DFT calculations showed that upon excitation the structure of the cationic $[Ag(Bipy)(POP)]^+$ complex remains practically unaffected and it is expected to exhibit a relatively small non-radiative decay with a large energy difference between the T_1 and S_0 states to almost 3 eV. The electronic spectrum of the complex exhibits absorption bands with a composite MLCT/LL′CT and IL character. A LEC device (ITO/PEDOT:PSS/Ag(I):[BMIM]PF_6/LiF:Ag) was fabricated that showed a wide emission with a turn-on voltage of ca. 4.5 V and maximum brightness of 395 $cd.m^{-2}$ at 5.5 V.

KEYWORDS: light-emitting electrochemical cells, electroluminescence, photoluminescence, Silver(I) complex, DFT calculations.

1. INTRODUCTION

Since their first utilization for light-emitting electrochemical cells (LECs)[1] copper (I) compounds have begun to attract more research and industrial interest in the field of light emitting devices[2] thanks to work conducted by McMillin *et al.*[3] for the preparation of copper(I) complexes with long-lived photoluminescence signals. The advantages of luminescent copper(I) materials of the general type [Cu(I)(N^N)(P^P)] (where N^N indicates a chelating diimine ligand, typically 1,10-phenanthroline and P^P denotes a bisphosphine ligand) are their ease of synthesis requiring only a few steps for the decoration of the ligand (N^N) and their ability to cover a wide region from the visible spectrum especially between red and green emissions. Moreover, copper is an inexpensive, abundant and environmentally friendly metal in comparison to iridium(III) and ruthenium(II) which are widely used for light-emitting electrochemical devices.[4] However, these copper materials suffer from several issues, for example, upon excitation the Cu(I), complex, which has a pseudo-tetrahedral geometry, oxidizes to a flatter Cu(II) complex, thus becoming susceptible to nucleophilic attack leading to an increase of non-radiative pathways and, consequently, dramatically reducing the luminescence properties. Additionally, when they are applied into a lighting device they are vulnerable to an irreversible process at high voltage leading to degradation. To overcome these issues, several research studies have been carried out to design new ligands that are capable of protecting the metal center and enhancing the luminescence properties.[5] Recently, it has been noted that a similar structure is possible with Ag(I) ion instead of Cu(I) as the metal center for similar complex structure.[6] Moudam *et al.*[7] demonstrated that the complex [Ag(I)(Bphen)(POP)]BF_4 with Bphen = 4,7-diphenyl-1,10-phenanthroline and POP = bis[(2-diphenylphosphino)phenyl]ether, exhibits good luminescence properties and was selected as a luminescent-down shifter for organic photovoltaics. Furthermore, the employment of homoleptic

silver(I)[8] and copper(I)[9] has been reported for organic light emitting diodes using poly(vinyl carbazole) (PVK) as a host hole transport material.

Out of interest, a new silver(I) complex [Ag(I)(Bipy)(POP)]BF_4 (with Bipy=2,2'-Bipyridine and POP ligands) was prepared as an active luminescent material for the first time in LEC technology. A LEC device (ITO/PEDOT:PSS/Ag(I):[BMIM]PF_6/LiF:Ag) was fabricated. The DFT calculations show that the complex exhibits absorption bands with a composite MLCT/LL′CT and IL character with an emission at yellow-greenish region.

2. RESULTS AND DISCUSSION

2.1. Synthesis and crystal structure of [Ag(Bipy)(POP)](BF$_4$) complex. The new silver complex [Ag(Bipy)(POP)](BF_4) was prepared according to a previously described procedure.[6,7] The white solid Ag(I) complex was obtained in good yield by the reaction of 2,2′-Bipyridine (Bipy) with stoichiometric quantities of bis[2-(diphenylphosphino)phenyl]ether (POP) and $AgBF_4$ in a mixture of chloroform: methanol (5:1) at 25°C as shown in the Supporting Information (Figure S1a). The complex was characterized in solution by ^{1}H NMR spectroscopy (Figure S1b). The $^{31}P\{^1H\}$ NMR spectra (Figure S1c) in $CDCl_3$ displays two doublets centered at δ = -7.08 ppm because of the coupling of the equivalent phosphorus atoms with both the ^{107}Ag (^1J = 366 Hz) and ^{109}Ag (^1J = 423 Hz) nuclei (for ^{107}Ag and ^{109}Ag, the natural abundance are 48.2 and 51.8%, respectively).[6,7]

The Ag(I) complex was characterized and its purity verified by elemental analysis. Crystals suitable for single crystal X-ray diffraction were obtained by slow diffusion from $CHCl_3$ solution. The ORTEP of the cationic moiety of the complex depicted in Figure 1 reveals a distorted tetrahedral coordination environment around Ag(I) central atom. It should be noted that the POP ligand is bound to the metal only through its pair of P donor atoms, the ether O atom being at a nonbonding distance from the Ag(I) metal center (>3.2 Å).

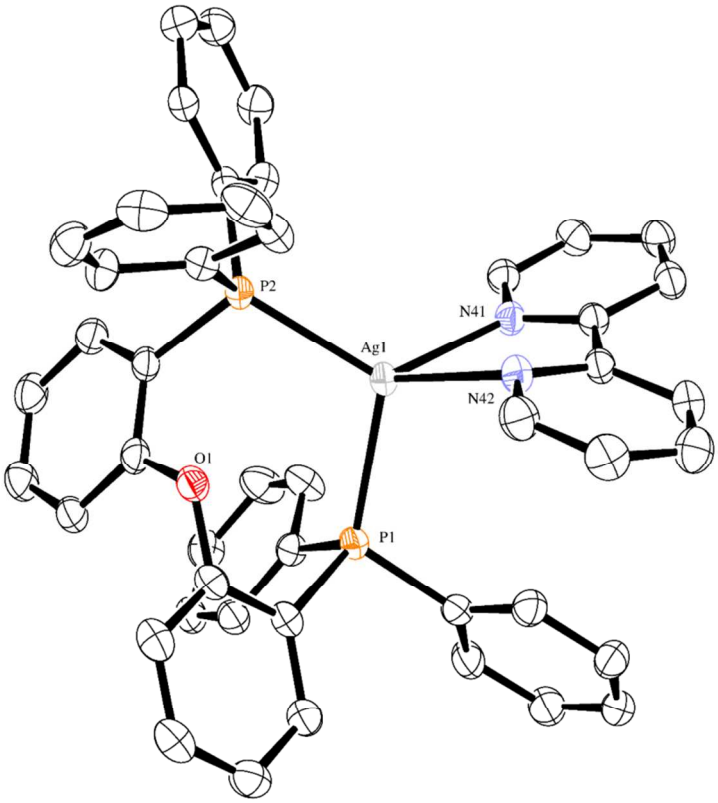

Figure 1. ORTEP with partial numbering of the cationic part of the [Ag(I)(Bipy)(POP)]BF_4 complex. The hydrogen atoms have been omitted for clarity. Thermal ellipsoids include 50% of the electron density.

In this complex, the silver atom is in an N2P2 distorted tetrahedral environment in which both the bipyridine and POP moieties are coordinated as chelating ligands. The Ag-N (2.328(2) Å, 2.394(2) Å) and Ag-P (2.4227(7) Å, 2.4961(7) Å) distances are within the normal range.[6] The distortion mainly arises from the restricted bite angle of the bipyridine ligand N(41)AgN(42) (70.84(8)°) and the corresponding diphosphine ligand P(1)AgP(2) (112.17(2)°).

Further distortion is observed within the bipyridine rings twisted by 23.6(1)° which is towards the upper end of observed twists for those in a similar chelating tetrahedral environment. [10] Additionally, the

angle of tilt for the bipyridine away from the defined NAgN plane at 17.1(1)° is only observed in a small percentage of structures. The bond lengths within the POP and bipyridine ligands compare well with values reported in the literature.[6] The aromatic rings are generally twisted with respect to each other, with none lying close enough for any possible π-π interactions. This is the result of the insertion of solvent molecules between two neighbouring POP ligands belonging to different cations, as shown in the SI (Figure S2). The shortest existing distance between the bipyridine plane and a solvent molecule (Cl of $CHCl_3$) is 3.8 Å. The BF_4 counter-anions are located nearest to the solvent molecules between the planes constituted by the cationic interacting moieties. The shortest distance between a fluorine atom and a proton of the POP is 2.3 Å.

2.2. Photoluminescence and DFT Computational Study. The electronic absorption and emission spectra of the Ag(I) complex are reported in Figure 2.

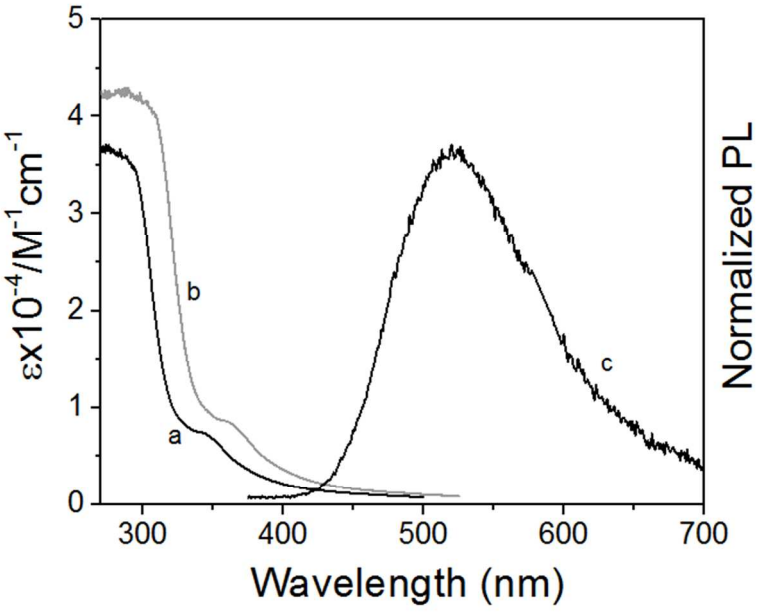

Figure 2. UV-vis absorption spectra of the [Ag(I)(Bipy)(POP)]BF_4 complex at room temperature (a) in PMMA film, (b) in dichloromethane, and (c) emission (λ_{exc} = 350nm) spectra of the [Ag(I)(Bipy)(POP)]BF_4 complex at room temperature in PMMA film.

The ligand-centered UV spectral feature and the broad MLCT band in the 325-400 nm spectral window is typical for a heteroleptic Ag(I) complex containing 4,7-diphenyl-1,10-phenanthroline (Bphen) and POP ligands.[7] The MLCT absorption band of the Ag(I) complex containing a POP unit occurs at higher energy which is likely to be related to the presence of electronegative P atoms as coordinative units, which tend to disfavor the electron donation to the bipyridine ligand by the Ag(I) central atom leading to an energy increase of MLCT transitions. Furthermore, the emission in PMMA of Ag(I) with POP and Bphen ligands described in ref. 7 is yellow with a maximum around 585 nm. In our case, when using the 2,2'-Bipyridine instead of 4,7-diphenyl-1,10-phenanthroline, the maximum of the emission is localized in the yellow-greenish region at 520 nm. Costa *et al.*[11] showed that the cationic $[Cu(Bipy)(POP)]^+$ complex exhibits an MLCT absorption at 398 nm and an emission in film around 610 nm. It is apparent that the MLCT and emission of the cationic $[Ag(Bipy)(POP)]^+$ complex are blue shifted and this should be related to the highest energy transition of the silver(I) in relation to copper(I) complexes which is due to the HOMO-LUMO excitations.

Table 1. Luminescence data of the $[Ag(I)(Bipy)(POP)]BF_4$ complex under different experimental conditions.

R.T. CH_2Cl_2			Solid State		
λ_{max}[a] [nm]	Φ_{em}[b] (%)	τ[c] [μs]	λ_{max}[a] [nm]	Φ_{em}[b] (%)	τ[c] [μs]
545	<0.01 (0.05)	[d] (46)	525	14	2.5

[a] Emission maxima from uncorrected spectra; in brackets, air free solutions, λ_{exc} = 350 nm. [b] Emission quantum yields in air-equilibrated and in air-purged solutions (in brackets). Standard used, $[Ru(bpy)_3]^{2+}$ in air equilibrated water (Φ = 0.028). [c] Excited state lifetimes in air-equilibrated and in air-purged solutions (in brackets). [d] Weak signal.

These results indicate that on passing from solution to solid state a significant spectral blue-shift by 20 nm is found (Table 1). This is a common behavior for charge transfer emission bands in rigid media. It is clear that, despite the weak emission in solution, the emission shows remarkable enhancement.

In order to get a deeper insight into the photophysical properties of the [Ag(Bipy)(POP)]BF_4 complex, we calculated the molecular, electronic and spectroscopic properties by a combined DFT/TD-DFT electronic structure calculation methodology. Figure 3 shows the molecular structures with selected structural parameters of the cationic $[Ag(Bipy)(POP)]^+$ complex in the ground singlet S_0 and the first triplet T_1 states optimized at the PBE0/TZP(Ag)∪ 6-31G(d,p)(E) level in the gas phase.

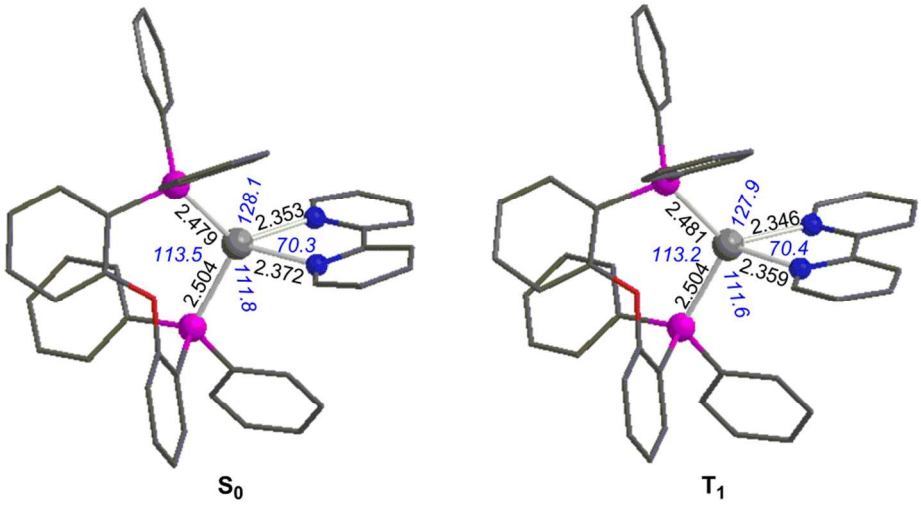

Figure 3. Equilibrium geometries of the $[Ag(Bipy)(POP)]^+$ cation in the S_0 (left) and T_1 (right) states, optimized at the PBE0/TZP(Ag)∪ 6-31G(d,p)(E) level in the gas phase.

Despite the packing forces in the crystal are not taken into account in the calculations, the gas phase calculated structural parameters are in good agreement with those obtained from the X-ray structural analysis of the complex. The calculated bond lengths are slightly elongated, by 0.03 - 0.06 Å (with the exception of one Ag-N bond calculated to be slightly shorter by 0.02 Å) while the calculated bond angles are slightly more obtuse by 0.6 - 5.3° (with the exception of one <N-Ag-N bond angle calculated

to be slightly more acute by 0.5 Å) as compared to the respective structural parameters determined by the X-ray crystallography. Noteworthy inclusion of the solvent effects ($CHCl_3$ solvent) in the calculation does not alter significantly the geometry of the $[Ag(Bipy)(POP)]^+$ cation in the S_0 ground state. The molecular structure of the $[Ag(Bipy)(POP)]^+$ complex optimized at the PBE0/TZP(Ag) ∪ 6-31G(d,p)(E) level in $CHCl_3$ solution is given in the SI (Figure S3) along with relevant structural parameters. Accordingly, only slight differences could be observed between the structural parameters calculated in the gas phase and the $CHCl_3$ solution.

To probe the emission process, we have also optimized the geometry of the $[Ag(Bipy)(POP)]^+$ cation in the first triplet excited state, T_1 (Figure 3). Remarkably, upon an $S_0 \rightarrow T_1$ excitation, the structure of the $[Ag(Bipy)(POP)]^+$ cation remains practically unaffected, since the changes in bond lengths and angles are in the ranges of 0.00 - 0.01Å and 0.1 - 0.3° respectively. Notice however, that there are some severe changes in dihedral angles upon the $S_0 \rightarrow T_1$ excitation, e. g. the dihedral angle between the pyridine rings changes by 14.7◦ while that between the chelate ligands changes by 44.6◦. In addition, the energy difference between the T_1 and S_0 states is quite large amounting to almost 3 eV (or more than 69 kcal/mol).

According to energy gap law the non-radiative decay rate constant, k_{nr} could be expressed as

$$k_{nr} = (T_m - S_o) \propto \{-\beta[E(T_m) - E(S_0)]\} \quad (1)$$

that is, the non-radiative decay rate of an excited state (T_m) increases as the energy difference between the m^{th} triplet excited state and the singlet ground state decreases. Parameter β is related to the structural distortion between the potential-energy surfaces of the T_m and S_0 states, and the larger the structural distortion, the faster the non-radiative decay. Therefore, based on the expression (1), the $[Ag(Bipy)(POP)]^+$ cation is expected to exhibit a relatively small non-radiative decay rate constant, k_{nr}

since its structural distortions upon $S_0 \rightarrow T_1$ excitation are very small. On the other hand, the $E(T_1)$ - $E(S_0)$ energy difference is quite large contributing also to the diminution of the k_{nr} constant.

Next, we have calculated the absorption spectra, in both the gas phase and $CHCl_3$ solution, by employing TD-DFT calculations at the PBE0/TZP(Ag)∪ 6-31G(d,p)(E) level of theory (Figure 4). The gas phase simulated absorption spectrum matches perfectly the experimentally derived absorption spectrum of the Ag(I) complex at room temperature in PMMA film. The simulated absorption spectrum in $CHCl_3$ solution is given in the SI (Figure S4).

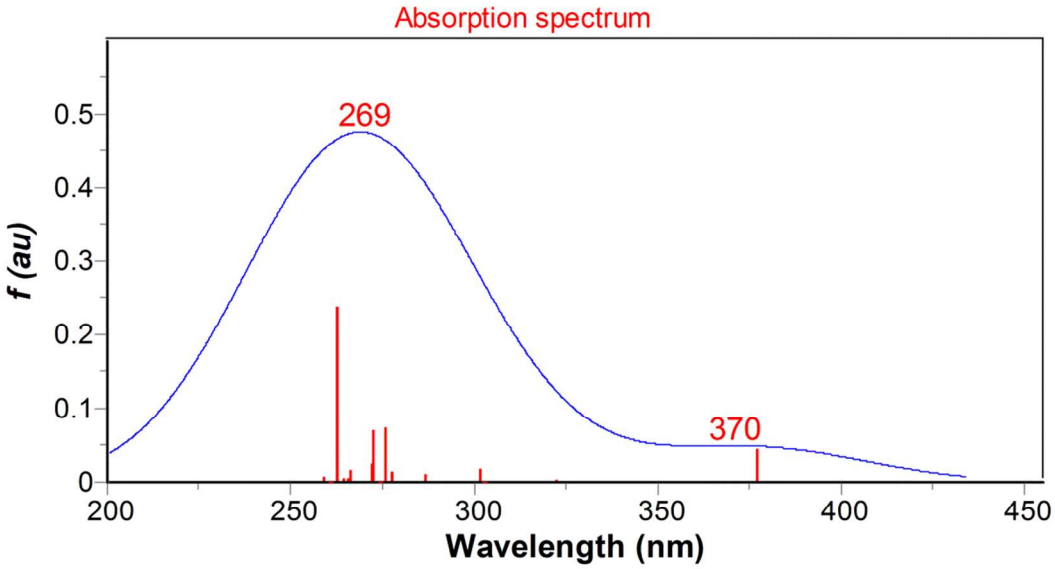

Figure 4. Gas phase absorption spectrum (FWHM=50) of the cationic $[Ag(Bipy)(POP)]^+$ complex, calculated at the TD-DFT/PBE0/TZP(Ag)∪ 6-31G(d,p)(E) level.

The gas phase simulated absorption spectrum exhibits one broad band peaking at 269 nm and a shoulder peaking around 370 nm in excellent agreement with experimental solid state absorption spectrum which also exhibits a broad band around 270 nm and a shoulder around 350 nm. Notice that, the inclusion of the solvent effects in the calculation, does not practically affect the simulated absorption spectrum of the cationic $[Ag(Bipy)(POP)]^+$ complex (Figure S4). Thus, the absorption spectrum of

$[Ag(Bipy)(POP)]^+$, in $CHCl_3$ solution, exhibits exactly the same qualitative features, while the main band and the shoulder peak at 270 and 355 nm, respectively, in excellent agreement with the experiment. The principal singlet-singlet electronic transitions in the absorption spectrum of the $[Ag(Bipy)(POP)]^+$ complex in the gas phase are collected in Table 2.

Table 2. Selected principal singlet-singlet optical transitions in the absorption spectrum of the $[Ag(Bipy)(POP)]^+$ complex calculated at the TD-DFT/PBE0/TZP(Ag)U6-31G(d,p)(E) level in the gas phase.

Electronic excitation (%composition)	E (eV)	λ (nm)	f (au)	μ
H-12 → L (51%), H-11 → L (15%)				
H-10 → L (6%), H-9 → L (6%)	4.717	263	0.239	2.064
H → L+4 (71%)	4.543	273	0.072	0.645
H → L+4 (90%)	4.492	276	0.075	0.683
H → L (99%)	3.286	377	0.046	0.576

The 3-D contour plots of the Highest Occupied Molecular Orbital (HOMO) and the Lowest Unoccupied Molecular Orbital (LUMO) are depicted schematically in Figure 5, while the 3-D contour plots of the rest of the MOs involved in the most important electronic transitions are given in the SI (Figure S5).

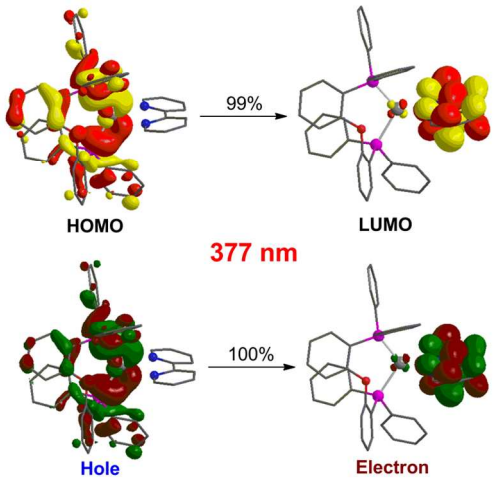

Figure 5. 3-D contour plots (isocontour of 0.03 au) of the HOMO and LUMO (top) and the Hole-Electron NTO pair (bottom) characterizing the electronic transition absorbing at 377 nm.

The shoulder appearing around 350 - 370 nm arises from the highest energy electronic transition at 377 nm which is due to the HOMO → LUMO excitation. Perusal of Figure 5 reveals that HOMO is mainly localized on the metal and to a lesser extent on one of the phenyl rings, while the LUMO is solely located on the bipyridyl ligand. Therefore, the shoulder appearing in the absorption spectrum could be characterized as Metal to Ligand Charge Transfer, MLCT as well as Ligand to Ligand Charge Transfer, LL′CT. In other words, the shoulder exhibits a composite MLCT/LL′CT character. The NTO analysis reveals that the excitation to the lowest singlet excited state, S_1 could be described by a single pair of Natural Transition Orbitals, NTOs (Figure 5) with shapes similar to those of the HOMO and LUMO. Thus, upon excitation to the first singlet excited state, the electron is located on the bipyridyl ligand, while the hole is mainly located on the metal as well as on one of the phenyl rings.

Next, the broad absorption band with maximum around 270 nm comprises a multitude of electronic transitions with the most intense appearing at 263, 273 and 276 nm (Table 2). The most intense electronic transition at 263 nm arises from a combination of excitations and based upon the MOs involved shown in the SI (Figure S5) could be assigned as LL′CT as well as intraligand, IL transition. The other two electronic transitions at 273 and 276 nm are due to a HOMO → LUMO+4 excitation and could be assigned as MLCT, for the LUMO+4 is mainly located on the (POP) ligand (Figure S5).

Finally the estimated vertical $S_0 \leftarrow T_1$transition energy of the $[Ag(Bipy)(POP)]^+$ complex is 2.45 eV (506 nm) in the gas phase calculations and 2.46 eV (504 nm) in the chloroform solution calculations, in good agreement with the experimental value of 2.38 eV (520 nm).

2.3. Light-emitting electrochemical device. The light-emitting electrochemical cell (LEC), a type of organic electroluminescent device, possesses many notable qualities for lighting display technology. The

main difference between OLEDs and LECs is that the active layer in the latter contains mobile ions. When the electroluminescent layer and the electrodes are not in contact, the ions reside in pairs. Upon application of an external bias over the electrodes, the cations and anions migrate towards the cathode and anode, respectively. In this manner, they screen the active material from the applied field and also establish very large electric fields within thin double layers at the electrode. When the applied voltage exceeds the potential corresponding to the band gap of the active material, the ionic double layers at the cathode and anode enable efficient injection of electrons and holes, respectively, into the semiconducting material. Subsequently, there is a redistribution of the ions in the layer in order to stabilize the electronic charge carriers, i.e. electrochemically doped regions are created. The injected electrons and holes migrate through the n-type and p-type doped regions towards each other and recombine to form an exciton, which releases its energy in the form of a photon.

In this type of device (Figure 6), the silver(I) complex is not doped in a semiconducting host polymer as for OLEDs. It is mixed with small amounts of the ionic liquid $[BMIM]^+[PF_6]^-$ (3-butyl-1-methylimidazolium hexafluorophosphate) which is known to improve the ionic conductivity inside the light-emitting layer due to its higher density of mobile ions and to reduce the aggregation and phase separation problems.[12]

We present a new iTMCs (ionic transition metal complexes) based LECs complex and the first example reported to date of a white LEC made with a charged $[Ag(I)(N^N)(P^P)]BF_4$ compound.

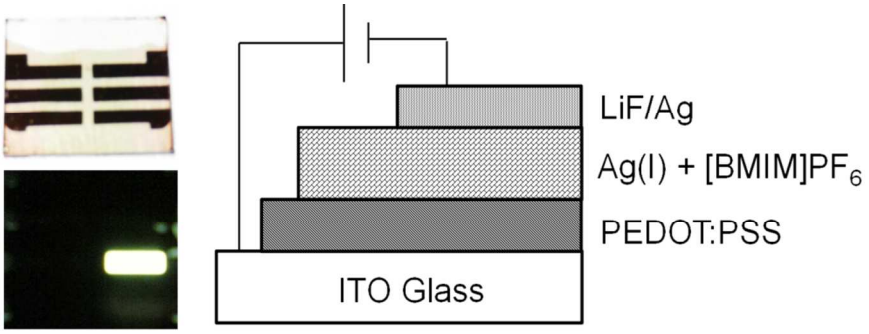

Figure 6. Device structure (layers are not on scale).

Based on the photoluminescence results and on the DFT calculations, the complex [Ag(Bipy)(POP)]BF_4 was selected for the fabrication of a light-emitting electrochemical device. The electroluminescence spectrum of the complex is significantly broader when compared to the photoluminescence spectrum recorded in PMMA. As a result, warm-white light was produced by the device. The current-voltage-brightness (*I-V-B*) characteristics (Figure 7) of the device indicate a turn-on voltage of ca. 4 V and maximum brightness of 395 cd.m^{-2} at 5.5 V. To the best of our knowledge, this is the first example of warm-white light emitting electrochemical with silver(I) complex as a triplet emitter, thus showing that silver(I) complexes are attractive candidates for light emitting applications.

Figure 8 shows the luminance and efficacy against voltage. The onset voltage is approximately 4.5V. A maximum efficacy is nearly 0.45 cd/A (5.5V) with a luminance efficiency of 54 cd/m^2 (9.4V). These efficiency is very similar to those obtained for the copper(I) LECs.[13] It should be improved by using appropriate hole and electron blocking layers in the device configuration.

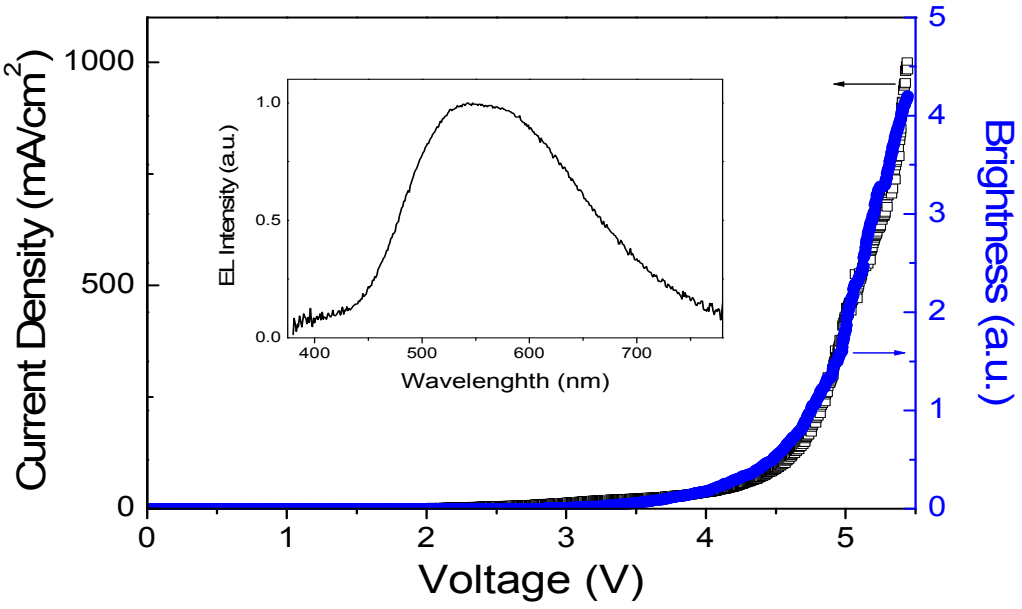

Figure 7. *I-V-B* characteristics of the device obtained from [Ag(Bipy)(POP)]BF_4. Inset: EL spectra of ITO/PEDOT:PSS/Ag(I):[BMIM]PF_6/LiF:Ag.

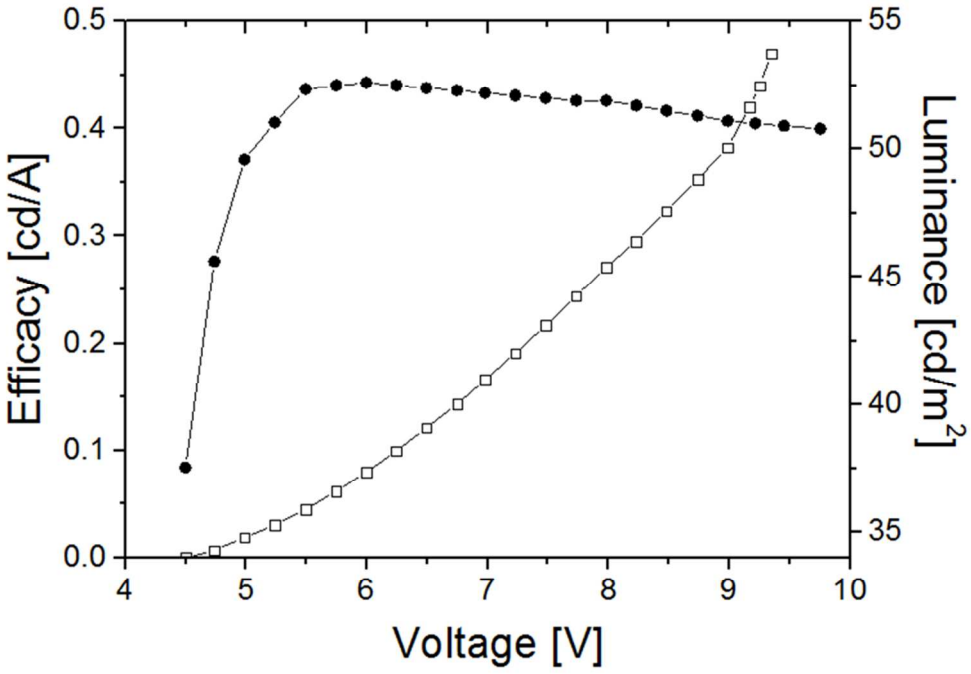

Figure 8. Efficacy (filled circles) and luminance (open squares) of the LEC device

3. CONCLUSIONS

In conclusion, we have described the first ionic transition-metal complexes (iTMCs) based on a $[Ag(I)(N^N)(P^P)]^+$ type complex as a promising phosphorescent emitter for light-emitting displays. A LEC device (ITO/PEDOT:PSS/Ag(I):[BMIM]PF_6/LiF:Ag) was fabricated with unexpected results showing a interesting emission properties. Remarkably, the DFT calculations show that upon an $S_0 \rightarrow T_1$ excitation, the structure of the cationic $[Ag(Bipy)(POP)]^+$ complex remains practically unaffected and it is expected to exhibit a relatively small non-radiative decay. This phenomenon is in contrast to the heteroleptic $[Cu(I)(N^N)(P^P)]^+$ complexes. In addition, the electronic spectrum of the complex exhibits absorption bands with a composite of MLCT/LL′CT and IL character and an emission at the yellow-

greenish region. The device brightness is moderate but it is clear from our study that there are easy routes to very simple Ag(I) complexes with highly emissive excited states and obvious potential for luminescence-based applications and devices.

4. EXPERIMENTAL

4.1. Synthesis of [Ag(Bipy)(POP)]BF_4. Silver tetrafluoroborate $AgBF_4$ (100 mg, 0.513 mmol) and bis[(2-diphenylphosphino)phenyl]ether (POP) (276 mg, 0.513 mmol) were dissolved in $CHCl_3$/MeOH (5:1) and stirred for 1 h, after which 2,2'-Bipyridine (Bipy) (80 mg, 0.513mmol) was added. This reaction mixture was stirred under argon at room temperature for 1h, before the mixture was evaporated and the complex [Ag(Bipy)(POP)]BF_4 was obtained in 85% yield as a solid white powder, which formed colourless crystals by slow evaporation from $CHCl_3$. ^{1}H NMR (400 MH, $CDCl_3$, δ): 6.81 (m, 4H), 7.00(t, J = 7.5 Hz, 2H), 7.12(m, 8H), 7.24(m, 10H), 7.34(m, 6H), 8.02(2t, J = 8 Hz, J = 8 Hz, 2H), 8.35(d, J = 8 Hz, 2H), 8.37(d, J = 4 Hz, 2H) ppm. ^{31}P{^{1}H} NMR (162 MHz, $CDCl_3$, δ): -7.08 (2d, $^1J^{31}_{P,}{}^{109}_{Ag}$ = 423 Hz, $^1J^{31}_{P,}{}^{107}_{Ag}$ = 366 Hz) ppm. Anal. Calcd for $C_{46}H_{36}AgBF_4N_2OP_2.2CHCl_3$: C 51.10, H 3.39, N 2.48; found C 51.21, H 3.41, N 2.41.

4.2. X-ray Crystallography. A suitable crystal was selected and data collected following a standard method,[14] on a Rigaku AFC12 goniometer at 100K equipped with an enhanced sensitivity (HG) Saturn724+ detector mounted at the window of an FR-E-Superbright molybdenum anode generator with HF Varimax optics (100μm focus). Cell determination, data collection, data reduction, cell refinement and absorption correction were carried out using CrystalClear.[15] Structure solution and refinement were carried out using SHELX programs.[16]

Crystal data for AgPOP : $C_{48}H_{38}AgBCl_6F_4N_2OP_2$, M = 1128.12, colourless block, a = 9.5560(7), b = 13.9607(10), c = 19.4900(14) Å, α = 100.126(6)°, β = 91.419(5)°, γ = 95.515(5)°, V = 2440.9(3) Å^3,

Triclinic, space group *P-1*, $Z = 2$, $\mu = 0.861$ mm^{-1}, reflections collected = 38260, independent reflections = 11101, $R_{int} = 0.0740$, $R1 = 0.0503$, $wR2 = 0.1334$ [$F^2 > 2\sigma(F^2)$], $R1 = 0.0553$, $wR2 = 0.1388$ (all data).

CCDC reference number 1404797, contains the supplementary crystallographic data for this paper. This data can be obtained free of charge from the Cambridge Crystallographic Data Centre via www.ccdc.cam.ac.uk/data_request/cif.

4.3. UV-vis and PL measurement. The absorption spectra were recorded with a UV-Vis-NIR (UV-3600 SHIMADZU), the photoluminescence was measured with Fluoromax-4 spectrophotometer with FluoroMax software from HORIBA Scientific equipped with a photomultiplier R928P as based detector for spectral coverage 200 nm–870 nm, (Wavelength Accuracy (± 0.5 nm)) with a Czerny-Turner monochromator. Thin film layer of [Ag(Bipy)(POP)]BF_4 in PMMA (1:5) with $CHCl_3$ was spin-coated at 3000 rpm for 1 min onto a quartz glass disc with 0.8 cm diameter. The film dried with Argon at room temperature for a few minutes to remove $CHCl_3$ and then the glass with the doped film was placed in a solid sample holder and transferred to the integrated sphere in the spectrophotometer for PL measurements.

Emission lifetimes were determined with the single photon counting technique by means of the same Edinburgh FLS920 spectrometer using a laser diode as excitation source (1 MHz, $\lambda_{exc} = 407$ nm, 200 ps time resolution after deconvolution). For solid samples, Φ_{em} have been calculated by corrected emission spectra obtained from an apparatus consisting of a barium sulphate coated integrating sphere (6 inches), an He-Cd laser (λ_{exc}: 325 nm, 5mW) as light source and a CCD AVA-Spec2048 as signal detector, following the procedure described by De Mello et al.[17]

4.4. Computational Details. Full geometry optimization without symmetry constrains were carried out in the gas phase and in $CHCl_3$ solution, for both the singlet ground state (S_0) and the lowest triplet excited state (T_1) of the cationic [Ag(Bipy)(POP)]$^+$ complex, using the full-range PBE0 non-local hybrid

GGA functional.[18-21] For the geometry optimizations we have used the TZP basis set of Jorge *et al.*[22] for the Ag atom and the Pople's 6-31G(d,p) split valence basis set for all other elements, E (the computational protocol is denoted hereafter as PBE0/TZP(Ag) ∪ 6-31G(d,p)(E). The choice of the PBE0 functional was based on our experience and the fact that PBE0 has been recognized to provide very accurate results for many molecular properties.[23] Moreover, the combination of PBE0 with TZP basis set for Ag(I) has been successfully applied in DFT calculations of silver(I) complexes.[24,25] The attainment of the energy minimum was verified by calculating the vibrational frequencies that result in the absence of imaginary eigenvalues. Time dependent density functional theory (TD-DFT)[26-28] calculations were performed at the same level i.e. by employing the PBE0/TZP(Ag)U6-31G(d,p)(E) computational protocol. The TD-DFT calculations were performed in the gas phase and in $CHCl_3$ solution for the singlet ground state (S_0) of the cationic $[Ag(Bipy)(POP)]^+$ complex including the lowest 20 singlet–singlet excitations. It should be noted that the TD-PBE0 excitation energies are, on the average, more accurate than those provided by other commonly used hybrid functional, such as B3LYP.[23,29] The vertical $S_0 \leftarrow T_1$ transition energy of the $[Ag(Bipy)(POP)]^+$ complex was calculated by single point DFT calculations at the same level of theory neglecting the energy loss by vibrational cooling. Despite the absence of adjustable parameters, besides providing a reliable description of the ground state properties of several classes of compounds TD-PBE0 provide also accurate results in the description of both the bright and dark excitation and both valence and Rydberg states.[23] Moreover, recent benchmark calculations of electronically excited states of organic compounds showed that the TD-PBE0-1/3 predict excitation states within an acceptable accuracy with respect to the symmetry-adapted cluster–configuration interaction (SAC–CI) method.[30]. All calculations were done using the Gaussian09, Rev. D.01 program suite.[31] Natural Transition Orbital analysis[32] was performed as implemented in the Gaussian09, Rev. D.01 software.

4.5. Fabrication of LEC devices. LEC device was initially prepared in a clean room environment using indium tin oxide (ITO) coated glass substrates, supplied by Psiotec ltd., UK, (R_s = 16 Ω/square) that was first cleaned using deionised water, acetone and isopropanol and blown dry using nitrogen, then treated in a UV-ozone reactor with oxygen plasma for 10 minutes. A layer of the conductive polymer PEDOT:PSS mixture (HC Starck Clevios PAI 4083) was spin coated (in air) onto ITO/glass substrate at 5000 rpm for 30s before a 20 min bake at 120°C on a plate to remove any residual H_2O. The device was fabricated in a glovebox, which maintained H_2O and O_2 concentrations to typically less than 0.1 part per million. On top of this layer the active film was deposited by spin-coating an acetonitrile solution of the complex [Ag(Bipy)(POP)]BF_4 with the ionic liquid in a molar ratio 4 to 0.5. A concentration of 20 mg mL^{-1} at 1000 rpm for 30 seconds leads to 100 nm thickness. The thickness of the film was determined using an Ambios XP1 profolimeter. Finally, a 5 nm layer of lithium fluoride (LiF) and a 100 nm layer of silver (Ag) were deposited by thermal evaporation through a shadow mask to form a composite cathode electrode, which defined six active areas of 0.2 cm^2. The measurement system used to characterize the devices consisted of a Newport simulator and a Botest GmbH SMU for taking *I-V-B* measurements. An Ocean Optics spectrometer with a sensor was used to measure the electroluminescence. The (x,y) Commission International de l'Eclairage (CIE) 1931 values for the sample were measured by Konika Minolta LS-100 luminance meter (with 1/3° acceptance angle and measuring brightness range from 0.01 to 999,900 cd/m^2).

ASSOCIATED CONTENT

Supporting Information

X-ray crystallographic files (CIF); tables of experimental data (PDF). This material is available free of charge via the Internet at http://rsc.org/advances.

ACKNOWLEDGMENTS

** Dr Omar Moudam acknowledge the financial support of EC through the Integrated Project from the Wales Ireland Network for Innovative Photovoltaic Technologies (WIN-IPT) project, funded through the Interreg 4A, Wales Ireland Programme 2007-13. The authors wish to thank Professor David R. McMillin for helpful discussion.

REFERENCES

(1) Armaroli, N.; Accorsi, G.; Holler, M.; Moudam, O.; Nierengarten, J.-F.; Zhou, Z.; Wegh, R. T.; Welter R. *Adv. Mater*. **2006**, *18*, 1313.

(2) www.cynora.com

(3) Cuttell, D. G.; Kuang S.-M.; Fanwick. P. E.; McMillin, D, R.; Walton, R. A. *J. Am. Chem. Soc*, **2002**, *124*, 6-7.

(4) Costa, D. R.; Ortí, E.; Bolink, H. J.; Monti. F.; Acorsi, G.; Armaroli, N. *Angew. Chem. Int. Ed*. **2012**, *51*, 8178-8211.

(5) Mohankumar, M.; Monti, F.; Holler, M.; Niess, F.; Delavaux-Nicot, B.; Armaroli, N.; Sauvage, J.-P.; Nierengarten, J.-F. *Chem. Eur. J*. **2014**, *20*, 12083.

(6) Kaeser, A.; Delavaux-Nicot,.B.; Duhayon, C.; Coppel, Y.; Nierengarten, J.-F. *Inorg. Chem*. **2013**, *52*, 14343.

(7) Moudam, O.; Bristow, N.; Chang, S.-W.; Horie, M.; Kettle, J. *RSC Adv*., **2015**, *5*, 12397.

(8) Kaeser, A.; Moudam, O.; Accorsi, G.; Séguy, I.; Navarro, J.; Belbakra, A.; Duhayon, C.; Armaroli, N.; Delavaux-Nicot, B.; Nierengarten, J.-F. *Eur. J. Inorg. Chem*. **2014**, 1345.

(9) Moudam, O.; Kaeser, A.; Delavaux-Nicot, B.; Duhayon, C.; Holler, M.; Accorsi, G.; Armaroli, N.; Séguy, I.; Navarro, J.; Destruel, P.; Nierengarten, J.-F. *Chem. Comm*., **2007**, 3077.

(10) Allen, F. H. *Acta. Cryst*., **2002** B58, 380.

(11) Costa, R. D.; Tordera, D.; Ortí, E.; Bolink, H. J.; Schönle, J.; Graber, S.; Housecroft, C. E.; Constable, E. C.; Zampese. J. A. *J. Mater. Chem*, **2011**, *21*, 16108.

(12) Su, H.-C.; Fang, F.-C.; Hwu, T.-Y.; Hsieh, H.-H.; Chen. H.-F.; Lee, G.-H.; Peng, S.-M.; Wong, K.-T.; Wu. C.-C. *Adv. Funct. Mater*. **2007**, *17*, 1019.

(13) Keller, S.; Constable, E. C.; Housecroft, C. E.; Neuburger. M.; Prescimone, A.; Longo, G.; Pertegás, A.; Sessolo, M.; Bolink, H. J. *Dalton Trans*, 2014, 43, 16593.

(14) Coles, S. J.; Gale, P. A. *Chem. Sci*., **2012,** *3*, 683.

(15) Rigaku, *CrystalClear- SM Expert 3.1 b27,* **2013**.

(16) Shedrick, G. M. *Acta Cryst*, **2015**, *C71*, 3.

(17) De Mello, J. C.; Wittmann, H. F.; Friend. R. H. *Adv. Mater*. **1997**, *9*, 230.

(18) Perdew, J. P.; Burke, K.; Ernzerhof, M. *Phys. Rev. Lett.* **1996**, *77*, 3865.

(19) Adamo, C.; Barone, V. *Chem. Phys. Lett.* **1997**, *274*, 242.

(20) Adamo, C.; Barone, V. *J. Chem. Phys.* **1999**, *110*, 6158.

(21) Ernzerhof, M.; Scuseria, G. E. *J. Chem. Phys.* **1999**, *110*, 5029.

(22) Campos, C. T.; Jorge, F. E. *Mol. Phys.* **2013**, *111*, 167.

(23) Improta, R. In *Computational Strategies for Spectroscopy: from Small Molecules to Nano Systems*, Ed. V. Barone, John Wiley & Sons Inc. Hoboken New Jersey 2012, pp 39-76.

(24) Reisinger, A.; Trapp, N.; Knapp, C.; Himmel, D.; Frank Breher, F.; Heinz Rüegger, H.; Krossing, I. *Chem. Eur. J.* **2009**, *15*, 9505.

(25) Damian, D.; Beck, J.; Decken, A.; Dionne, I.; Schmedt auf der Gunne, J.; Hoffbauer, W.; Köchner, T.; Krossing, I.; Passmore, J.; Rivard, E.; Steden, F.; Wang, X. *Dalton Trans.***, 2011,** *40*, 5865.

(26) Van Gisbergen, S. J. A.; Kootstra, F.; Schipper, P. R. T.; Gritsenko, O. V.; Snijders, J. G.; Baerends, E. J. *Phys. Rev. A: At., Mol., Opt. Phys.* **1998**, *57*, 2556.

(27) R. Bauernschmitt, R. Ahlrichs, R. *Chem. Phys. Lett.* **1996**, *256*, 454.

(28) Jamorski, C.; Casida, M. E.; Salahub, D. R. *J. Chem. Phys.*, **1996**, *104*, 5134.

(29) Conzalez, L.; Escudero, D.; Serrano-Andres, L. *Chem. Phys. Chem.* **2012**, *13*, 28.

(30) Allpour, M. *Theor. Chem. Acc.* **2015**, *134*, 70.

(31) Frisch, M. J.; et al., Gaussian 09, Revision D.01; Gaussian, Inc.: Wallingford, CT, 2010.

(32) Martin, R. L. *J. Chem. Phys.*, **2003**, *118*, 4775.

Graphical abstract:

First Light-Emitting Electrochemical Cell with [Ag(I)(N^N)(P^P)] type Complex**

Omar Moudam,[a]* *Athanassios C. Tsipis,*[b]* *Srikanth Kommanaboyina,*[c] *Peter N. Horton,*[d] *Simon J. Coles*[d]

[a]School of electronic engineering, University of Bangor, Dean St, LL57 1UT, Bangor, UK, E-mail: o.moudam@bangor.ac.uk, omoudam@yahoo.co.uk
[b]Laboratory of Inorganic and General Chemistry, Department of Chemistry, University of Ioannina, 451 10 Ioannina, Greece, E-mail: attsipis@uoi.gr
[c]School of Chemistry, University of Bangor, LL57 2UW, Bangor, UK
[d]EPSRC National Crystallography Service, School of Chemistry, University of Southampton, Highfield, Southampton, SO17 1BJ, UK

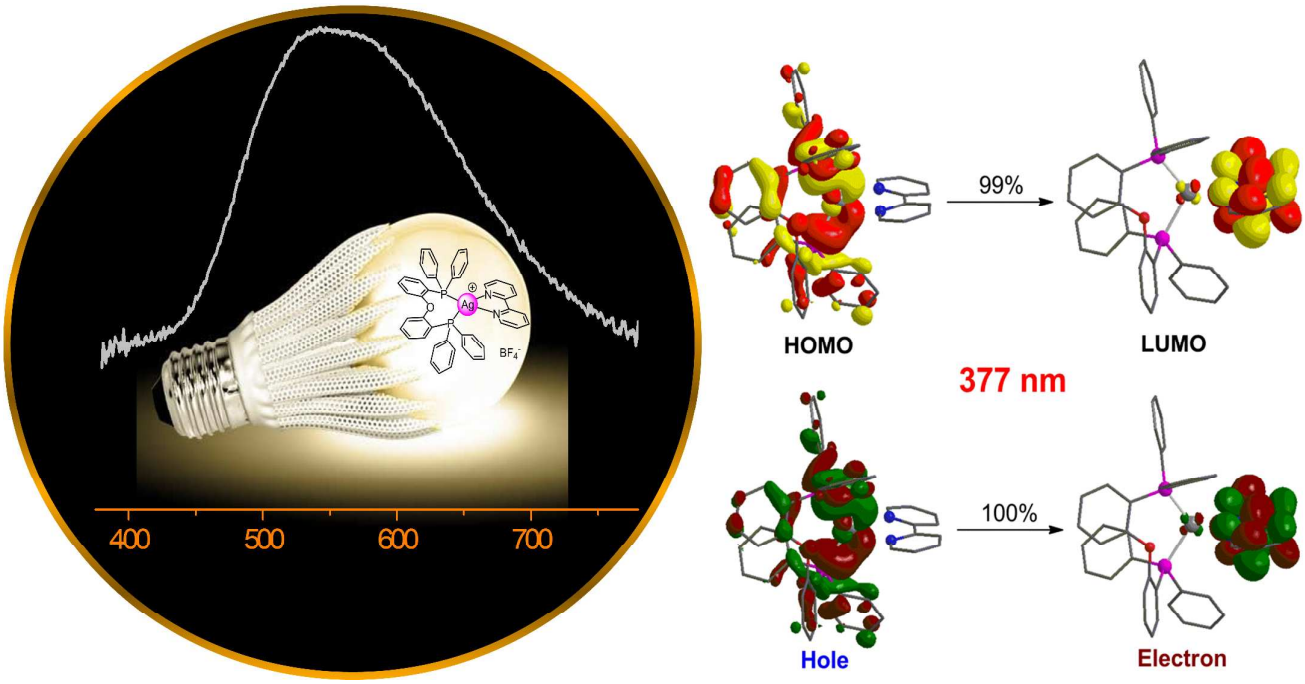

First Light-Emitting Electrochemical Cell with [Ag(I)(N^N)(P^P)] type Complex